Materials and Design 180 (2019) 107904

Contents lists available at ScienceDirect

Materials and Design

journal homepage: www.elsevier.com/locate/matdes

Multi-objective optimization of composite plates using lamination parameters

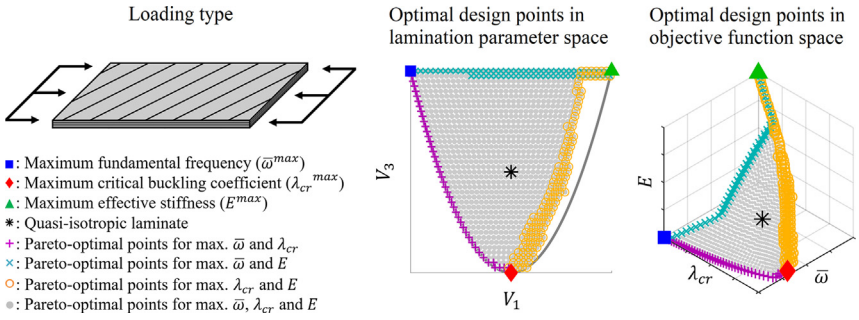
Gokhan Serhat *, Ipek Basdogan

Koc University, College of Engineering, Department of Mechanical Engineering, Istanbul 34450, Turkey

HIGHLIGHTS

- Multi-objective optimization of composite plates is performed using lamination parameters.
- Fundamental frequency, buckling load and effective stiffness metrics are maximized.
- Pareto-optimal solutions are determined considering various problem cases.
- A valuable insight has been provided on conformity/conflict of multiple objectives.
- Presented methodology can be utilized for the optimal design of laminated plates.

GRAPHICAL ABSTRACT



ARTICLE INFO

Article history:
Received 17 April 2019
Received in revised form 27 May 2019
Accepted 28 May 2019
Available online 3 June 2019

Keywords:
Laminated composite plates
Multi-objective optimization
Lamination parameters
Fundamental frequency
Buckling load
Effective stiffness

ABSTRACT

Laminated composite plates are extensively used in various industries due to their high stiffness-to-weight ratio and directional properties that allow optimization of the stiffness characteristics for specific applications. In multi-objective optimization problems, optimal designs for individual performance metrics may be conflicting, necessitating knowledge on the design requirements for different metrics and potential trade-offs. In this paper, a multi-objective design methodology for laminated composite plates with dynamic and load-carrying requirements is presented. Lamination parameters are used to characterize laminate stiffness matrices in a compact form resulting in a convex design space. Single and multi-objective optimization studies are carried out to determine the optimal stiffness properties. For improving the dynamic performance, maximization of the fundamental frequency metric is aimed. For enhancing the load-carrying capability, buckling load and equivalent stiffness metrics are maximized. Conforming and conflicting behavior of multiple objective functions for different plate geometries, boundary conditions and load cases are presented by determining Pareto-optimal solutions. The results provide a valuable insight for multi-objective optimization of laminated composite plates and show that presented methodology can be used in the design of such structures for improving the dynamic and load-carrying performance.

© 2019 Published by Elsevier Ltd. This is an open access article under the CC BY-NC-ND license (http://creativecommons.org/licenses/by-nc-nd/4.0/).

1. Introduction

Optimal design of composite plates for the best operational performance is an important engineering problem. Because of their high stiffness-to-weight ratio, composite materials have gained popularity

* Corresponding author at: Max Planck Institute for Intelligent Systems, Haptic Intelligence Department, Stuttgart 70569, Germany.
E-mail address: gserhat13@ku.edu.tr (G. Serhat).

https://doi.org/10.1016/j.matdes.2019.107904
0264-1275/© 2019 Published by Elsevier Ltd. This is an open access article under the CC BY-NC-ND license (http://creativecommons.org/licenses/by-nc-nd/4.0/).

in the industry over the last couple of decades. Fiber-reinforced laminated composites offer the possibility of optimizing the stiffness properties as an additional advantage due to their directional structure. Stiffness properties of these materials can be tailored to yield the optimal response for the desired application. In multi-objective optimization problems, the optimal designs for different performance metrics may be conflicting. Therefore, it is essential to develop methodologies for multi-objective optimization of composite laminated plates to determine the optimal parameters in the given design space.

Many composite stacking-sequence optimization studies are concerned with increasing fundamental frequency, buckling load and effective stiffness. Maximization of the fundamental frequency is used to reduce the dynamic response amplitudes of the structures excited with the frequencies up to the fundamental frequency. Increasing buckling load is an important criterion used in the design of plate structures carrying compressive loads. Maximizing the overall stiffness is essentially equivalent to reducing the maximum strain which is a common design objective used to enhance the integrity of load-carrying structures. In particular cases, simultaneous consideration of a multiple of aforementioned metrics is required to improve both dynamic and load-carrying performances. For instance, in the design of aircraft panels, maximization of fundamental frequency, buckling load and effective stiffness can be all important.

There are many available optimization studies which take maximization of the fundamental frequency as the design objective. For instance, Bert [1] developed a closed-form formula for simply-supported thin rectangular laminated plates based on the classical lamination theory. He used it to maximize the fundamental frequency of symmetric and balanced laminates by choosing fiber orientation angles as design variables. Narita and Robinson [2] conducted a layerwise optimization to obtain the maximum fundamental frequency for laminated composite panels using Ritz method to calculate the natural frequencies. Apalak et al. [3] calculated the fundamental frequencies of laminated composite plates using an artificial neural network model which is trained by finite element analyses. They utilized a genetic algorithm to find optimal laminate configurations providing maximum frequencies for various edge conditions.

Optimization of composite panels to increase buckling load is also extensively covered in the literature. Hirano [4] analyzed laminated plates with orthotropic, equally thick layers subjected to uni-axial and bi-axial compression. He computed optimal layer angles maximizing critical buckling load using an analytical relation for different panel aspect ratios, number of layers and load ratios. Hu and Lin [5] investigated the effects of panel aspect ratio and boundary conditions on buckling optimization of symmetrically laminated plates. They used finite element analyses and sequential linear programming method to calculate the optimal responses. Erdal and Sonmez [6] determined optimum laminate stacking-sequences for maximum laminate buckling load capacity using analytical expressions together with simulated annealing algorithm. They were able to obtain a number of coequal optimal designs using the search algorithm which circumvents termination at the local minima.

Overall stiffness maximization of laminated composites is similarly investigated by many researchers. For example, Kam and Lai [7] maximized the stiffness of laminated composite plates by determining the optimal fiber angles and layer thicknesses. In their work, they used shear deformable finite elements and augmented Lagrangian method for optimization. Gürdal et al. [8] introduced the concept of using curvilinear fibers within the laminates which allows variable-stiffness properties. They employed a uni-directional variation based on a linear function to define the fiber orientation angles of the individual layers. For flat rectangular composite laminates, they calculated overall panel stiffness and buckling load for different design parameters to demonstrate the trade-off between these responses.

In several studies, lamination parameters are used as design variables instead of number of layers, layer angles, and thicknesses to formulate the problem in a more compact way and avoid local optima. For maximization of the fundamental frequency, Fukunaga et al. [9] performed layup optimization of symmetrically laminated plates based on classical laminated plate theory (CLPT) by formulating the responses in terms of lamination parameters. Diaconu et al. [10] conducted a similar study for thick panels by using First-order Shear Deformation Theory (FSDT) and compared the results with the ones obtained via CLPT. Serhat and Basdogan [11] calculated the fundamental frequency contours of curved panels in lamination parameter plane using finite element analyses. They investigated the combined effects of panel aspect ratio, curvature and boundary conditions on the maximum frequency points. Abdalla et al. [12] also used lamination parameters in their optimization study to maximize the fundamental frequency of variable-stiffness laminated plates. Serhat and Basdogan [13] proposed a methodology based on lamination parameters for designing flat and curved variable-stiffness laminates. They utilized the method for the maximization of fundamental frequency and showed that variable-stiffness designs outperform the constant-stiffness ones. Considering buckling, Fukunaga et al. [14] obtained the contours of uni-axial and shear buckling loads for square plates, on the feasible region of lamination parameter plane. Grenestedt [15] found optimal lamination parameters providing maximum buckling load for shear panels of various aspect ratios. Ijsselmuiden et al. [16] also used lamination parameters to maximize buckling load but they extended the approach for variable-stiffness panels. Regarding the maximum effective stiffness requirements, Fukunaga and Sekine [17] demonstrated the contours of in-plane and coupling stiffness components for symmetric laminates as a function of lamination parameters. They also proposed a method for determining laminate configurations corresponding to the lamination parameters. Miki and Sugiyama [18] used lamination parameters for optimal stiffness design of orthotropic laminates. They showed contour plots of strain energy within the feasible design space for plates undergoing bending due to centrally applied concentrated load. They also calculated optimal laminate configurations providing maximum bending stiffness as a function of plate aspect ratio. Setoodeh et al. [19] investigated the optimal design of fiber reinforced rectangular composite plates for minimum compliance design problem for variable-stiffness laminates in lamination parameters space. They showed that significant improvements in stiffness can be obtained compared to constant-stiffness designs by using variable-stiffness laminates.

In multi-objective optimization studies, different metrics frequently require different optimal designs. On this matter, several multi-objective laminate optimization studies have been conducted to improve both dynamic and load-carrying performance. For instance, Kam and Chang [20] performed a layerwise optimization study to find maximum buckling load and maximum vibration frequency for thick laminated composite plates using FEM together with weighted-sum optimization method. They investigated effects of side-to-thickness ratio, aspect ratio and numbers of layers for simply-supported symmetrically and antisymmetrically laminated plates exposed to uni-axial compression. Abouhamze and Shakeri [21] also used weighted-sum method for the maximization of first natural frequency and critical buckling load of cylindrical panels. One shortcoming of weighted-sum optimization is obtaining only a single solution instead of a set of nondominated solutions. As a more general approach, Nik et al. [22] carried out optimization studies to find Pareto-optimal solutions for maximizing overall stiffness and buckling load of a composite laminate plate with curvilinear fiber paths by varying the fiber orientations. They demonstrated the conflicting behavior of overall stiffness and buckling load when they are used together as the performance metrics. As a preliminary investigation, a multi-objective optimization study in lamination parameters domain was conducted by the authors of current study [23]. They maximized fundamental frequency and effective stiffness using weighted-sum approach as the optimization technique.

Although Pareto-optimal solutions for multi-objective optimization of fiber-reinforced composites have been studied in the literature, to

the best of the authors' knowledge, lamination parameters have not been used as the parametrization technique in the existing studies. In this study, a multi-objective design optimization framework for dynamic and load-carrying requirements of laminated composite plates is introduced. Laminate stiffness properties are represented and optimized using lamination parameters as design variables. Maximization of the fundamental frequency, buckling load, and effective stiffness are chosen as the design objectives. Pareto-optimal solutions are determined for the first time for different combinations of design objectives using lamination parameters. Two different panel aspect ratios and three different load cases are considered. The results are visualized on Miki's lamination diagram to provide an insight into potential solutions for multi-objective optimization problems. Significant changes in the trends of the optimal solutions in the lamination parameters domain are demonstrated for different problem types. The organization of this study is as follows: Section 2 covers the problem description including plate model, load cases, and responses. In Section 3, single-objective optimization results are presented and discussed. Section 4 contains multi-objective optimization results. Conclusions and directions for future activities are outlined in Section 5.

2. Problem description

2.1. Structural model

In the analyses, basic rectangular flat plates have been used to determine fundamental relations between the selected performance metrics. The schematic diagram of the plate model with length a, width b, total thickness h and layer angles $\pm\theta$ is shown in Fig. 1. Simply-supported and clamped boundary conditions are considered. The laminate is assumed to be balanced and symmetric.

2.2. Lamination parameters

2.2.1. Formulation

Lamination parameters were initially proposed by Tsai and Hahn [24]. They allow compact representation of the laminate configuration by approximating the overall stiffness properties in terms of material invariants and lamination parameters. Instead of the number of plies, their relative thicknesses, and orientation angles; the lamination parameters can be used as the design variables. Another attractive feature of lamination parameters is their convex solution space shown by Grenestedt and Gudmundson [25], which generally eliminates local optimality problems except for a few response types such as forced vibration response [26].

Using the CLPT, the constitutive equations for a laminated composite plate are defined as [27]:

$$\begin{Bmatrix} N_x \\ N_y \\ N_{xy} \\ M_x \\ M_y \\ M_{xy} \end{Bmatrix} = \begin{bmatrix} A & B \\ B & D \end{bmatrix} \begin{Bmatrix} \varepsilon_x^0 \\ \varepsilon_y^0 \\ \varepsilon_{xy}^0 \\ \kappa_x \\ \kappa_y \\ \kappa_{xy} \end{Bmatrix} \tag{1}$$

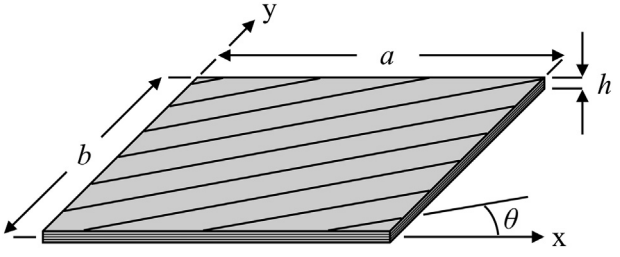


Fig. 1. Laminated composite plate.

where N_x, N_y and N_{xy} are the force resultants per unit depth; M_x, M_y and M_{xy} are the moment resultants per unit depth; ε_x^0, ε_y^0 and ε_{xy}^0 are the mid-plane strains; κ_x, κ_y and κ_{xy} are the plate curvatures. A, B and D are in-plane stiffness, in-plane/bending coupling and bending stiffness tensors, respectively, which can be formulated in terms of the lamination parameters and material invariants. For balanced and symmetric laminated plates, it is possible to model normalized in-plane stiffness tensor using only two lamination parameter variables as follows [27]:

$$\frac{A}{h} = \begin{bmatrix} U_1 & U_4 & 0 \\ U_4 & U_1 & 0 \\ 0 & 0 & U_5 \end{bmatrix} + \begin{bmatrix} U_2 & 0 & 0 \\ 0 & -U_2 & 0 \\ 0 & 0 & 0 \end{bmatrix} V_1 + \begin{bmatrix} U_3 & -U_3 & 0 \\ -U_3 & U_3 & 0 \\ 0 & 0 & -U_3 \end{bmatrix} V_3 \tag{2}$$

where V_i are the normalized lamination parameters:

$$V_1 = \frac{1}{h}\sum_{k=1}^{N_l} t_k \cos 2\theta_k$$

$$V_3 = \frac{1}{h}\sum_{k=1}^{N_l} t_k \cos 4\theta_k \tag{3b}$$

N_l, t_k and θ_k are number of layers, layer thicknesses and layer angles, respectively. U_i are the material invariants calculated using the following equation [10]:

$$\begin{Bmatrix} U_1 \\ U_2 \\ U_3 \\ U_4 \\ U_5 \end{Bmatrix} = \begin{bmatrix} 3/8 & 3/8 & 1/4 & 1/2 \\ 1/2 & -1/2 & 0 & 0 \\ 1/8 & 1/8 & -1/4 & -1/2 \\ 1/8 & 1/8 & 3/4 & -1/2 \\ 1/8 & 1/8 & -1/4 & 1/2 \end{bmatrix} \begin{Bmatrix} Q_{11} \\ Q_{22} \\ Q_{12} \\ Q_{66} \end{Bmatrix} \tag{4}$$

where Q_{ij} are the reduced stiffness matrix entities given by

$$\begin{Bmatrix} Q_{11} \\ Q_{22} \\ Q_{12} \\ Q_{66} \end{Bmatrix} = \begin{Bmatrix} E_1/\gamma \\ E_2/\gamma \\ \nu_{12}E_2/\gamma \\ G_{12} \end{Bmatrix} \tag{5}$$

Here, E_1, E_2, G_{12} and ν_{12} are elastic modulus in the fiber direction, elastic modulus perpendicular to the fiber direction, in-plane shear modulus and major Poisson's ratio of a uni-directional composite layer, respectively. $\gamma = (1 - \nu_{12}\nu_{21})$ where reciprocity relations for orthotropic layers require minor Poisson's ratio to be: $\nu_{21} = \nu_{12}E_2/E_1$. For symmetric laminates in-plane/bending coupling tensor is zero. Additionally, when the laminate consists of a large number of balanced layers distributed homogenously through the thickness, bending stiffness matrix satisfies the relation: $D = Ah^2/12$. Therefore, similar to A, D also becomes a function of V_1 and V_3 [28]. This is the assumption adopted in this study which eliminates bending-twisting coupling and results in a reduced design space for D.

2.2.2. Miki's lamination diagram

Miki's Lamination Diagram is a graphical tool to visualize the feasible domain of the balanced and symmetric laminates [29]. In Fig. 2, the diagram is illustrated with exemplary points for [0°], [±45°], and [90°] and [0° ±45° 90°] (quasi-isotropic) laminates. The horizontal axis V_1 and the vertical axis V_3 are the normalized lamination parameters. All the feasible design points need to be within the diagram. The lower part of the feasible domain is bounded by the curve: $V_3 = 2{V_1}^2 - 1$. Every point on this curve is only achievable by a balanced symmetric laminate with one distinct angle defined by

$$\theta = \frac{\cos^{-1}(V_1)}{2} \tag{6}$$

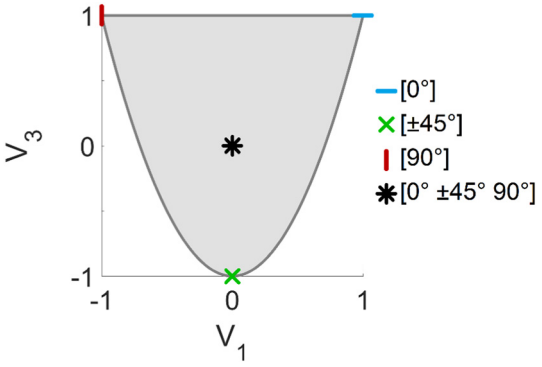


Fig. 2. Miki's lamination diagram.

The upper part is bounded by $V_3 = 1$ line. The points on this line can be obtained by different combinations of 0° and 90° layers.

2.3. Performance metrics

In this paper, two of the responses: fundamental natural frequencies and critical buckling coefficients are computed by using the developed in-house finite element analysis (FEA) software. This FEA framework allows establishing the connection between lamination parameters and nodal stiffness matrices and performing the analyses repeatedly for various cases. In the laminate modeling, 4-noded rectangular isoparametric Mindlin shell elements, which can carry both in-plane and bending loads are used. The analyses are performed to obtain solutions for different plate aspect ratios, stiffness properties and boundary conditions. For effective stiffness calculations, analytical relations available in the literature are used.

2.3.1. Fundamental frequency

Following element formulation, discretization, and assembly processes; Newton's second law provides the following system of equations:

$$Ku + M\ddot{u} = f \tag{7}$$

where K is the global stiffness matrix, M is the global mass matrix; u, $\ddot{u}$ and f are the nodal displacement, acceleration and force vectors, respectively. Then, the natural frequencies of the plate (ω_n) and corresponding mode shape vectors (u_n) can be obtained by solving Eqs. (8) and (9), respectively [30]:

$$\det(K - \omega_n{}^2 M) = 0 \tag{8}$$

$$(K - \omega_n{}^2 M)u_n = 0 \tag{9}$$

The calculated frequency values are normalized using the frequency parameter $\overline{\omega}$ defined as [9].

$$\overline{\omega} = \frac{\omega_n b^2}{\pi^2 h}\sqrt{\frac{12\rho}{Q_{22}}} \tag{10}$$

where ρ is laminate density.

2.3.2. Buckling load

In buckling analyses, initially geometric stiffness matrix K_g is computed using the stress field obtained for the selected loading type. After that, the buckling parameter λ_b can be obtained by solving the eigenvalue equation [31]:

$$\det(K - \lambda_b K_g) = 0 \tag{11}$$

The minimum eigenvalue is the critical buckling coefficient λ_{cr} which depends on plate aspect ratio, loading case and material properties. The true buckling load can be obtained by multiplying the critical buckling coefficient and the loading magnitude. Therefore, for unit loading, the buckling load is equal to the λ_{cr} value. Note that, the sign of $\lambda_b K_g$ in Eq. (11) is determined with respect to the convention for the prestresses so that the calculated buckling load is positive.

2.3.3. Effective stiffness

In lamination parameters domain, effective material stiffnesses (equivalent moduli) in the x and y-directions (E_x^0 and E_y^0) can be obtained by using (−) and (+) signs for (±)'s in Eq. (12), respectively, which is given as follows [27]:

$$\frac{E_x^0 + E_y^0}{2} \pm \frac{E_y^0 - E_x^0}{2} = \frac{U_1{}^2 - U_5{}^2 - U_2{}^2 V_1{}^2 + 2(U_1 + U_5)U_3 V_3}{U_1 \pm U_2 V_1 + U_3 V_3} \tag{12}$$

Similarly, effective shear stiffness can be written as

$$G_{xy}^0 = U_5 - V_3 U_3 \tag{13}$$

For the calculations, the stiffness metrics are normalized as $E_x = E_x^0/E_1$, $E_y = E_y^0/E_2$ and $G_{xy} = G_{xy}^0/G_{12}$. For uni-axial loading in x-direction, the minimization of strains essentially implies maximization of Ex_x, which is the stiffness in the loading direction. Similarly, bi-axial loading with $N_x/N_y = 1$ requires maximizing the normalized mean stiffness: $\overline{E} = (E_x + E_y)/\max(E_x + E_y)$. To attain minimum shear strain under uniform shear stress, G_{xy} is maximized.

3. Single-objective optimization

In general, gradient-based optimization algorithms work very well with the lamination parameter formulation due to convex nature of the design space. However, in addition to determining the optimal design points, obtaining the response contours is also aimed in this study to provide a broader insight. For this reason, a full-factorial search with a resolution of 0.05 in the lamination parameter variables is applied ensuring the complete exploration of the design space with 1141 points over the feasible domain.

In this section, the results regarding single-objective optimization of composite panels are presented. Each performance metric is investigated for the simply-supported and clamped panels with two different panel aspect ratios. In addition, different load cases are considered for maximum critical buckling coefficient and maximum effective stiffness metrics. The panel thickness-to-length ratio (h/a) is held constant at 0.01 complying with the thin plate assumption. The plate material is chosen as carbon fiber-reinforced epoxy with the properties given in Table 1 [9]. The response data obtained for individual metrics is also used as the input for the multi-objective optimization studies performed in the next section.

3.1. Fundamental frequency maximization

In the following, the maximum value of fundamental frequency is searched. Fig. 3 shows the non-dimensional fundamental natural frequency contours for a balanced and symmetric plates as a function of lamination parameters V_1 and V_3 for different aspect ratios and

Table 1
Material properties of uni-directional carbon-epoxy composite laminate.

E_1 (GPa)	142.0
E_2 (GPa)	10.8
G_{12} (GPa)	5.49
ν_{12}	0.3
ρ (kg/m^3)	1.6

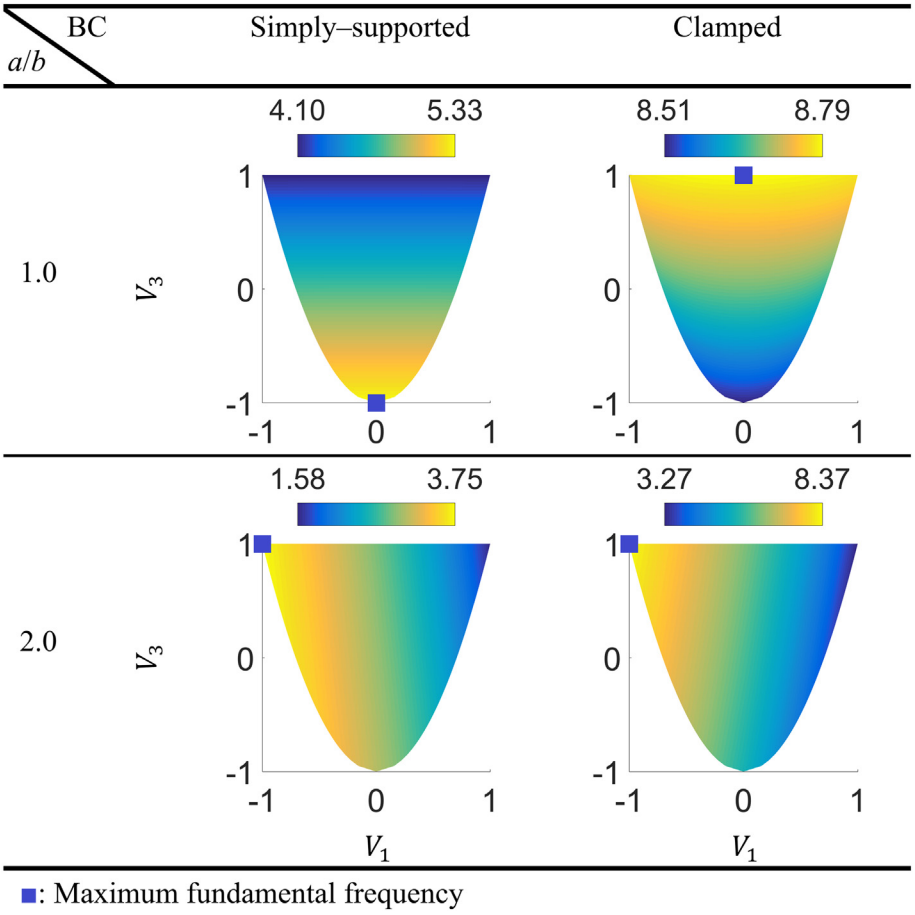


Fig. 3. Fundamental frequency parameter $\overline{\omega} = \omega_n b^2 \sqrt{12\rho/Q_{22}}/(\pi^2 h)$ contours on lamination parameter plane for simply-supported and clamped panels with different aspect ratios.

boundary conditions. The contour plots agree with the ones presented in [9]. One should note the convex nature of the response surfaces resulting from modeling in lamination parameters domain. The maximum fundamental frequency points are indicated by blue squares ■). The results show the trends of the simply-supported and clamped panel contours are opposite for $a/b = 1.0$, where they are very similar for $a/b = 2.0$. This is because, when aspect ratio is increased, the influence of constraining the rotational degrees-of-freedom on boundaries gets smaller. In addition, when a/b ratio is 1.0, the change in the frequency values for the clamped plate is considerably smaller compared to the simply-supported plate. This is because, the stiffening effect of the boundary conditions is significantly more dominant than the stiffening due to the fiber orientations for square plates [32]. Table 2 shows the calculated optimal values and the ones from [9] presented for validation purposes, where the variables at the optimum points are denoted by "*opt*" superscript. The results are in almost perfect agreement. The small differences are attributed to the use of different numerical solution methods, as the results have been obtained by using Rayleigh-Ritz method for simply-supported edges and Galerkin method for clamped edges in reference [9]. When the optimal solutions lie on the lower boundary of Miki's lamination diagram, they can only be obtained by specific layer angles which can be calculated using Eq. (6). In such instances, the optimal laminate angles (θ^{opt}'s) are also presented in the results together with optimal lamination parameters. In the current case, the optimum angle for $a/b = 1.0$ is 45° for simply-supported panels. However, for clamped panels, the optimum point lies on the upper boundary which cannot be obtained by single-angle laminates. For $a/b = 2.0$, 90° laminates are required for both boundary conditions which is a common result for high aspect ratio panels [32]. The fundamental mode shapes for the maximum fundamental frequency designs are shown in Fig. 4.

3.2. Buckling load maximization

For the buckling analyses, 3 different unit load cases are considered: uni-axial loading, bi-axial loading with $N_x/N_y = 1$ and shear loading

Table 2
Optimal design points yielding maximum fundamental frequency values and corresponding layer angles for simply-supported and clamped panels with different aspect ratios.

a/b		BC							
		Simply-supported				Clamped			
		V_1^{opt}	V_3^{opt}	$\pm\theta^{opt}$	$\overline{\omega}^{opt}$	V_1^{opt}	V_3^{opt}	$\pm\theta^{opt}$	$\overline{\omega}^{opt}$
1.0	Present FE	0.0	−1.00	45°	5.33	0.0	1.00	N.A.	8.79
	Ref. [9]	0.0	−1.00	45°	5.32	0.0	1.00	N.A.	8.77
2.0	Present FE	−1.00	1.00	90°	3.75	−1.00	1.00	90°	8.37
	Ref. [9]	−1.00	1.00	90°	3.73	−1.00	1.00	90°	8.31

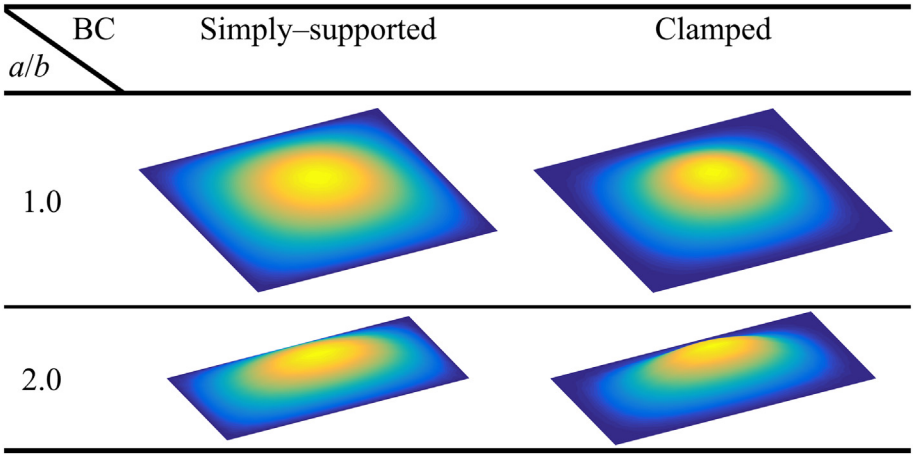


Fig. 4. Fundamental mode shapes of simply-supported and clamped panels with different aspect ratios for the maximum fundamental frequency designs.

which are illustrated in Fig. 5. The critical buckling coefficient contours for simply-supported panels are presented in Fig. 6. The results for different aspect ratios and loading conditions are grouped in the rows and the columns, respectively. The sharp changes occurring on the responses originate from the change of buckling modes characterized by the number of half-waves in x and y-directions denoted by *m* and *n*,

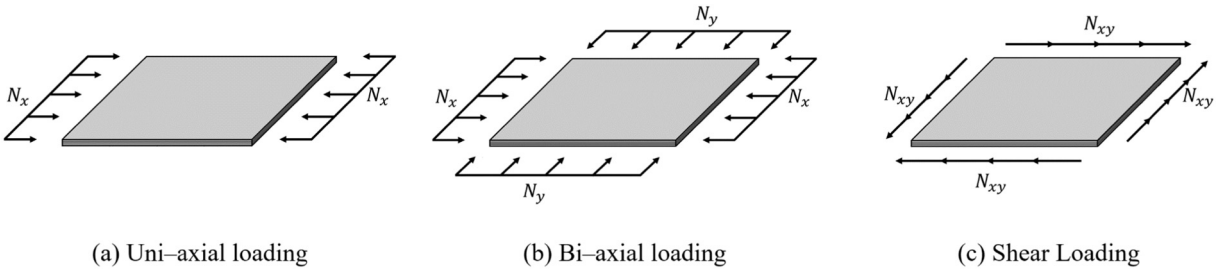


Fig. 5. Load cases used for the buckling analyses.

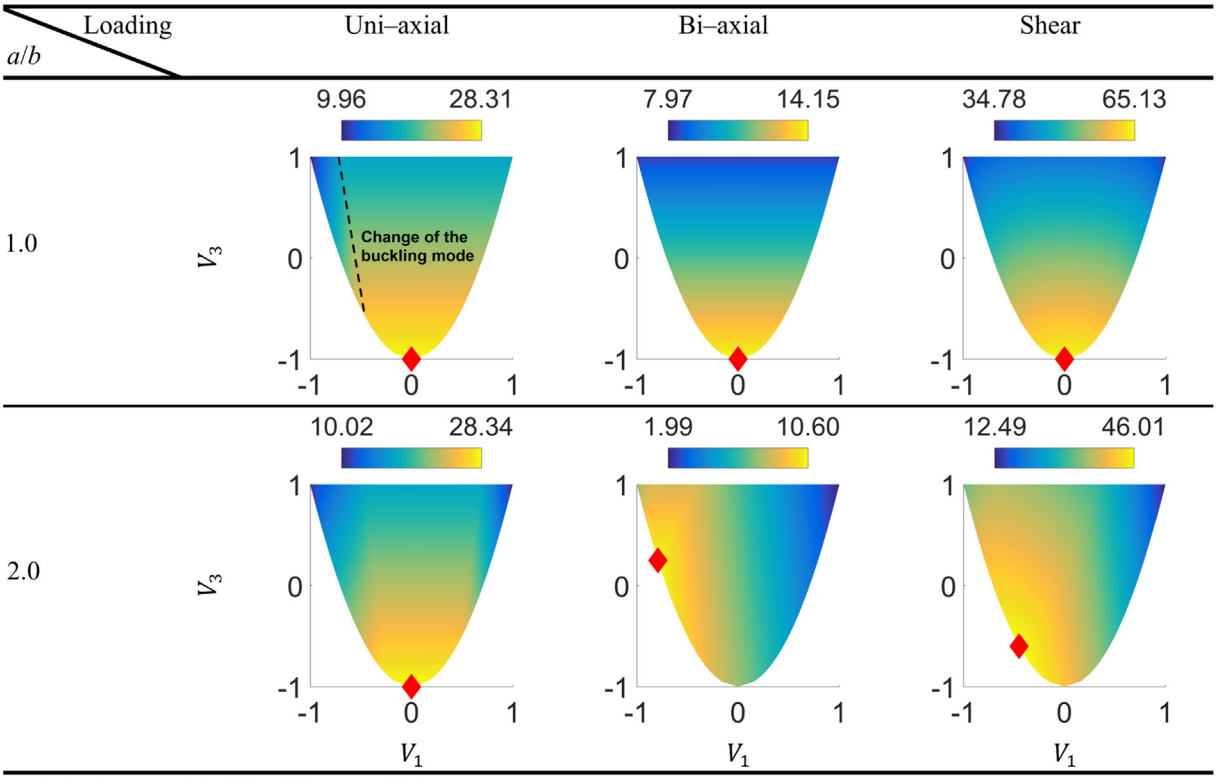


Fig. 6. Critical buckling coefficient contours in lamination parameter plane for simply-supported panels subjected to different loadings.

Table 3
Optimal design points yielding maximum critical buckling coefficient values and corresponding layer angles for simply-supported panels of different aspect ratios.

a/b		Loading											
		Uni-axial				Bi-axial				Shear			
		V_1^{opt}	V_3^{opt}	$\pm\theta^{opt}$	$\lambda_{cr}{}^{opt}$	V_1^{opt}	V_3^{opt}	$\pm\theta^{opt}$	$\lambda_{cr}{}^{opt}$	V_1^{opt}	V_3^{opt}	$\pm\theta^{opt}$	$\lambda_{cr}{}^{opt}$
1.0	Present FE	0.0	−1.0	45°	28.31	0.0	−1.0	45°	14.15	0.0	−1.0	45°	65.13
	Ref. [14]	0.0	−1.0	45°	28.30	N.A.	N.A.	N.A.	N.A.	0.0	−1.0	45°	63.88
2.0	Present FE	0.0	−1.0	45°	28.34	−0.791	0.250	71.1°	10.60	−0.447	−0.600	58.3°	46.01
	Ref. [14]	0.0	−1.0	45°	28.30	N.A.	N.A.	N.A.	N.A.	−0.391	−0.695	56.5°	44.61

respectively. For example, for $a/b = 1.0$ and uni-axial loading, buckling occurs with $(m = 2, n = 1)$ at the area lying on the left side of the dashed line, where at the other region it occurs with $(m = 1, n = 1)$. For square under bi-axial loading the contour plot is insensitive to the change of V_1 but solely changes with V_3. The reason for such behavior is that the system is symmetric in terms of both geometry and loading. For simply-supported boundary conditions, the displacement field can be written as the multiplication of the sinusoidal terms along x and y-coordinates. The resulting solutions contain the sum of D matrix entities for both buckling load [6] and fundamental frequency [1] (note that top-left response surface in Fig. 3 is similar). V_1 is only present in the first two diagonal terms of D, and the sum of V_1 contributions in these terms is zero. Therefore the solutions become solely linear functions of V_3.

The optimum points resulting in maximum buckling load are denoted by red diamonds (♦). The values of the design parameters and responses at the optimum points are tabulated in Table 3 together with the results from [14]. As the results show, all load cases require $(V_1^{opt} = 0.0, V_3^{opt} = -1.0)$ as optimal solution which is the same point yielding the maximum fundamental frequency for the simply-supported square panel. However, for $a/b = 2.0$, the optimum point changes for bi-axial and shear loading cases conforming to results of [14].

Fig. 7 shows the critical buckling modes for the simply-supported panels with the maximum buckling load designs. The buckling mode shapes for uni-axial and bi-axial loading are the same for $a/b = 1.0$, but they are all different for $a/b = 2.0$.

Fig. 8 and Table 4 show the critical buckling coefficient contours and tabulated optimal results for clamped panels, respectively. The results demonstrate the significant changes in the critical buckling coefficient contours and the optimal designs occurring with the alteration of the boundary conditions.

Fig. 9 shows the critical buckling modes for the clamped panels with the maximum buckling load designs. Unlike simply-supported plates, the buckling mode shapes under uni-axial and bi-axial loading are the same for clamped plates with both $a/b = 1.0$ and $a/b = 2.0$.

3.3. Effective stiffness maximization

Fig. 10 shows the contours of effective stiffnesses: E_x, $\overline{E}$ and G_{xy} in lamination parameter plane. The optimal solutions are marked by green triangles (▲), and their values are tabulated in Table 5. The optimum points for E_x and G_{xy} are $(V_1^{opt} = 1.0, V_3^{opt} = 1.0)$ and $(V_1^{opt} = 0.0, V_3^{opt} = -1.0)$ which correspond to 0° and ±45° laminates, respectively. For $\overline{E}$, the optimum is located at $(V_1^{opt} = 0.0, V_3^{opt} = 1.0)$ which is only obtainable by cross-ply laminates with equal proportions of 0° or 90° layers.

4. Multi-objective optimization

In multi-objective optimization studies, it is common that different objectives functions require different optimal designs. In such cases, the best compromises among all the possible designs should be found. When the objectives are functions of only a single design variable, the set of best (non-dominated) design points forms the curve named Pareto front [33]. The best design points imply that the value of an objective in the set cannot be further improved without worsening at least one other objective value. Depending on the priorities, any point on the Pareto set can be regarded as the optimum. For the functions of two variables, Pareto sets generally appear as a surface in parameter space. In objective function space, Pareto fronts typically take the form of a surface when 3 objectives are considered.

In this section, multi-objective optimization results for combinations of maximum fundamental frequency, maximum critical buckling coefficient, and maximum effective stiffness are presented. By

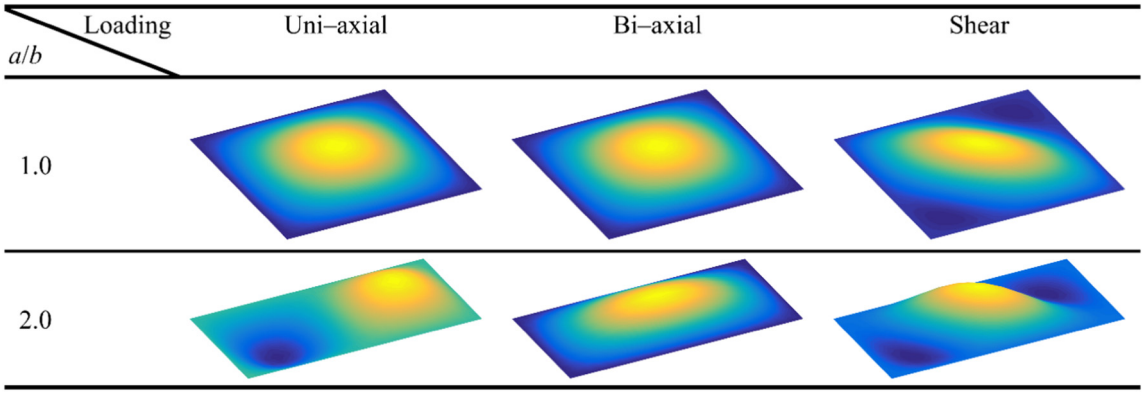


Fig. 7. Critical buckling modes for the simply-supported panels with the maximum buckling load designs.

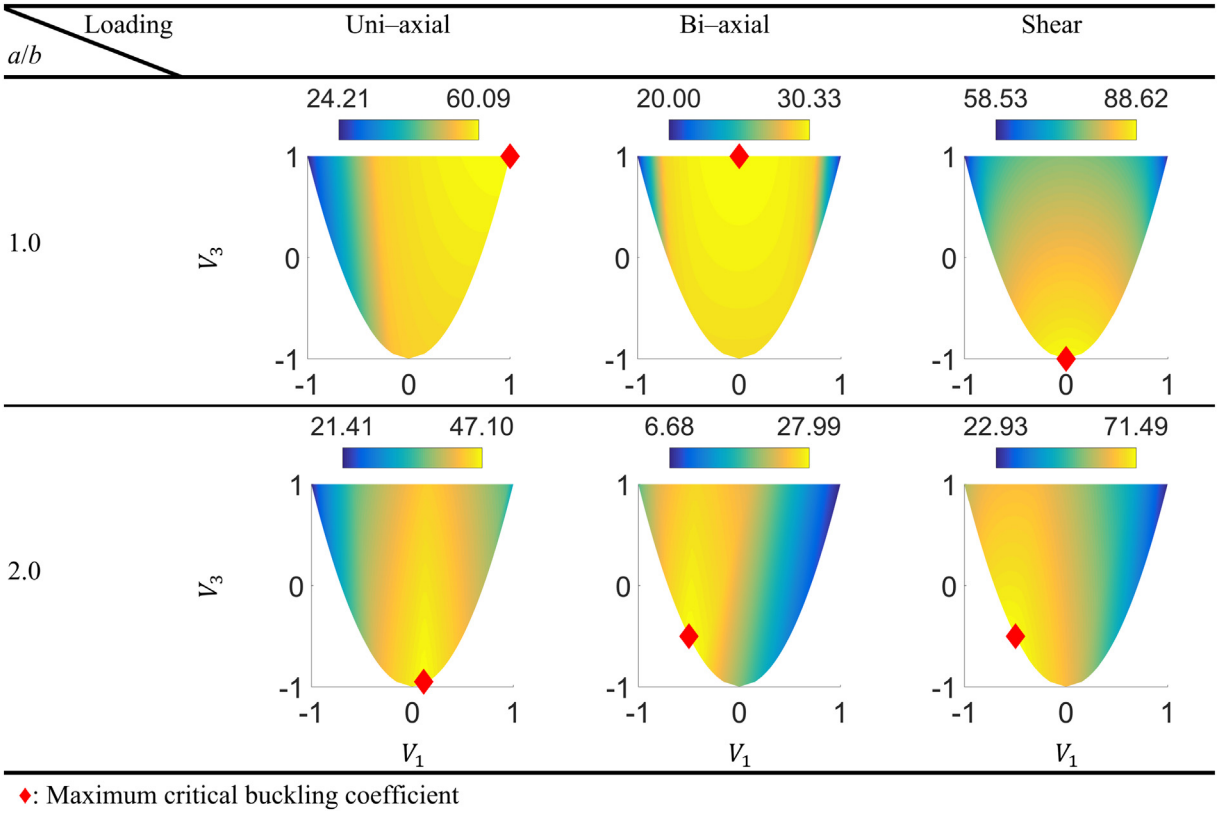


Fig. 8. Critical buckling coefficient contours in lamination parameter plane for clamped panels subjected to different loadings.

Table 4
Optimal design points yielding maximum critical buckling coefficient values and corresponding layer angles for clamped panels of different aspect ratios.

a/b		Loading											
		Uni-axial				Bi-axial				Shear			
		V_1^{opt}	V_3^{opt}	$\pm\theta^{opt}$	${\lambda_{cr}}^{opt}$	V_1^{opt}	V_3^{opt}	$\pm\theta^{opt}$	${\lambda_{cr}}^{opt}$	V_1^{opt}	V_3^{opt}	$\pm\theta^{opt}$	${\lambda_{cr}}^{opt}$
1.0	Present FE	1.0	1.0	0°	60.09	0.0	1.0	N.A.	30.33	0.0	−1.0	45°	88.62
	Ref. [14]	1.0	1.0	0°	59.66	N.A.	N.A.	N.A.	N.A.	0.0	−1.0	45°	89.08
2.0	Present FE	0.113	−0.950	41.8°	47.10	−0.500	−0.500	60°	27.99	−0.500	−0.500	60°	71.49
	Ref. [14]	0.108	−0.977	41.9°	47.39	N.A.	N.A.	N.A.	N.A.	−0.503	−0.494	60.1°	69.17

using the response data over the lamination parameter domain as the input for the optimization framework, Pareto-optimal solutions are determined for each binary combinations of objectives and for all three objectives.

4.1. Simply-supported panels

Fig. 11 shows Pareto-optimal points for maximum fundamental natural frequency, buckling coefficient and effective stiffness considering

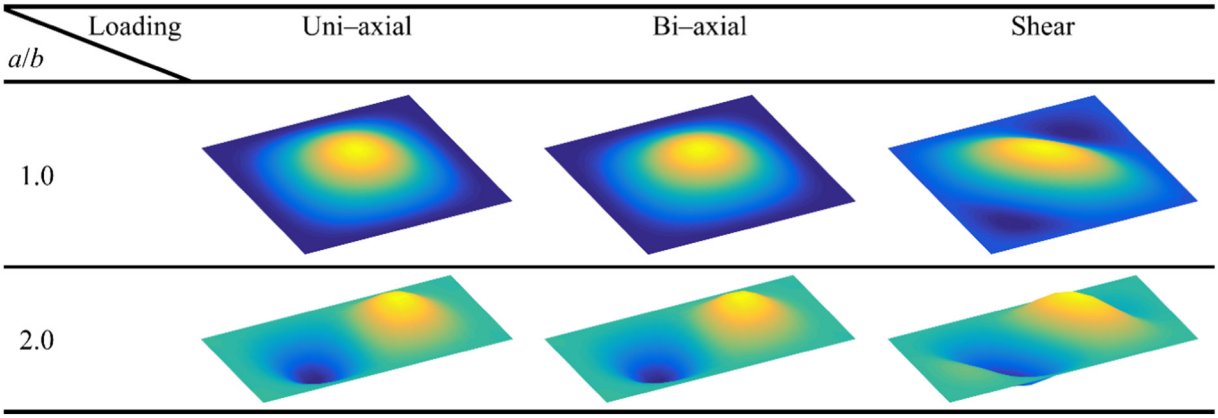


Fig. 9. Critical buckling modes for the clamped panels with the maximum buckling load designs.

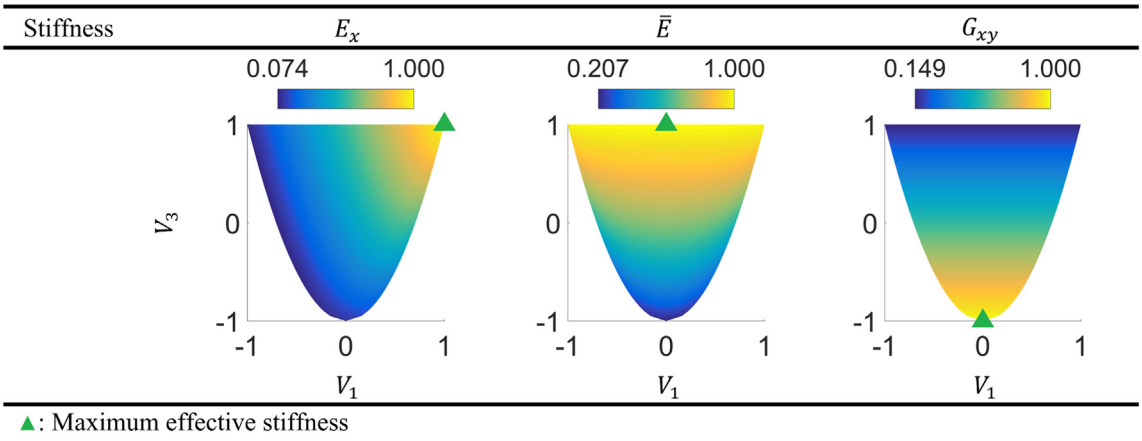


Fig. 10. Contours of effective stiffnesses: E_x, $\overline{E}$ and G_{xy} in lamination parameter plane.

Table 5
Optimal design points yielding maximum effective stiffness values and corresponding layer angles.

Stiffness	E_x				$\overline{E}$				G_{xy}			
	V_1^{opt}	V_3^{opt}	$\pm\theta^{opt}$	${E_x}^{opt}$	V_1^{opt}	V_3^{opt}	$\pm\theta^{opt}$	$\overline{E}^{opt}$	V_1^{opt}	V_3^{opt}	$\pm\theta^{opt}$	${G_{xy}}^{opt}$
	1.0	1.0	0°	1.0	0.0	1.0	N.A.	1.0	0.0	−1.0	45°	1.0

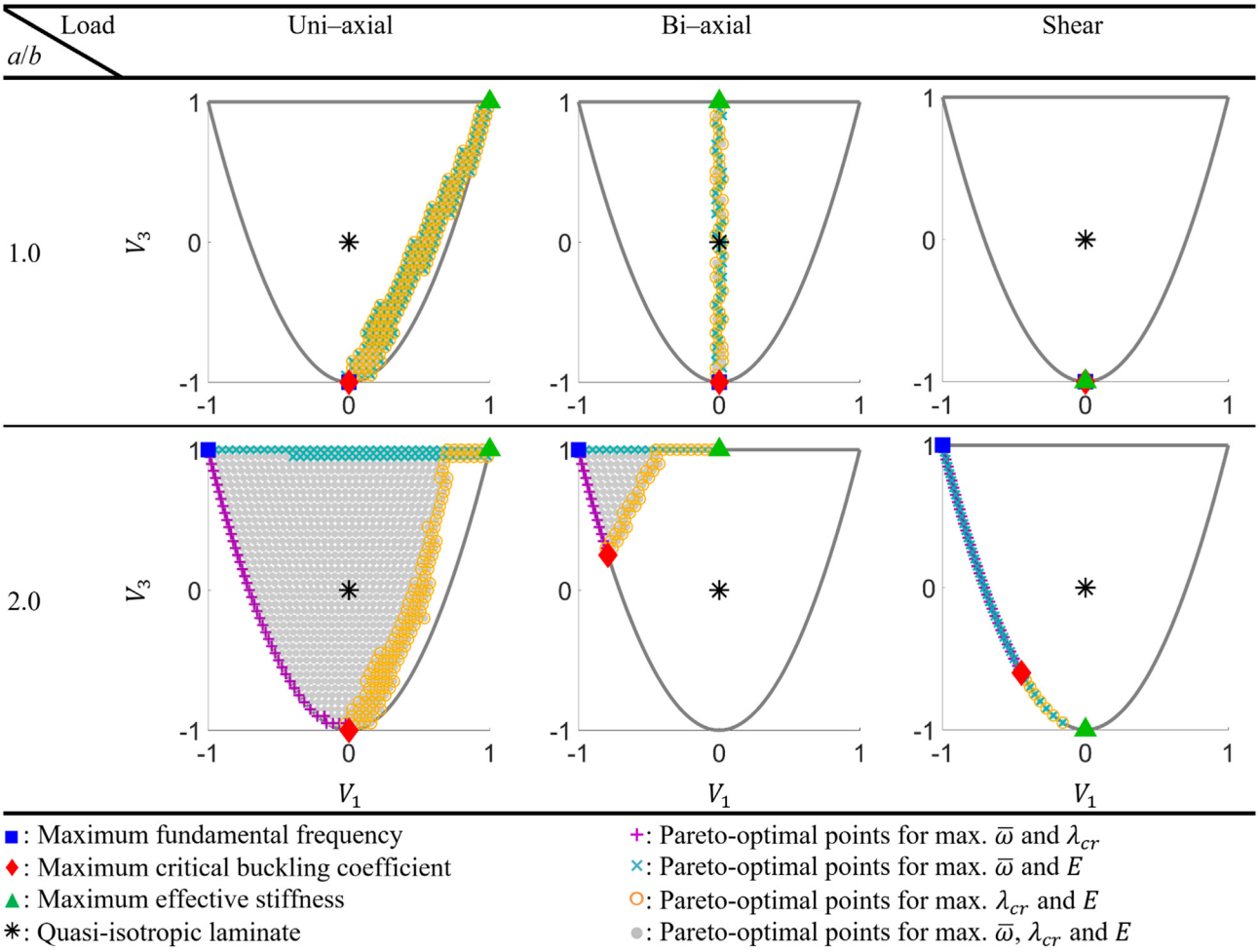


Fig. 11. 2-objective and 3-objective Pareto-optimal design points for maximum fundamental frequency, critical buckling coefficient and effective stiffnesses considering simply-supported panels subjected to different loadings.

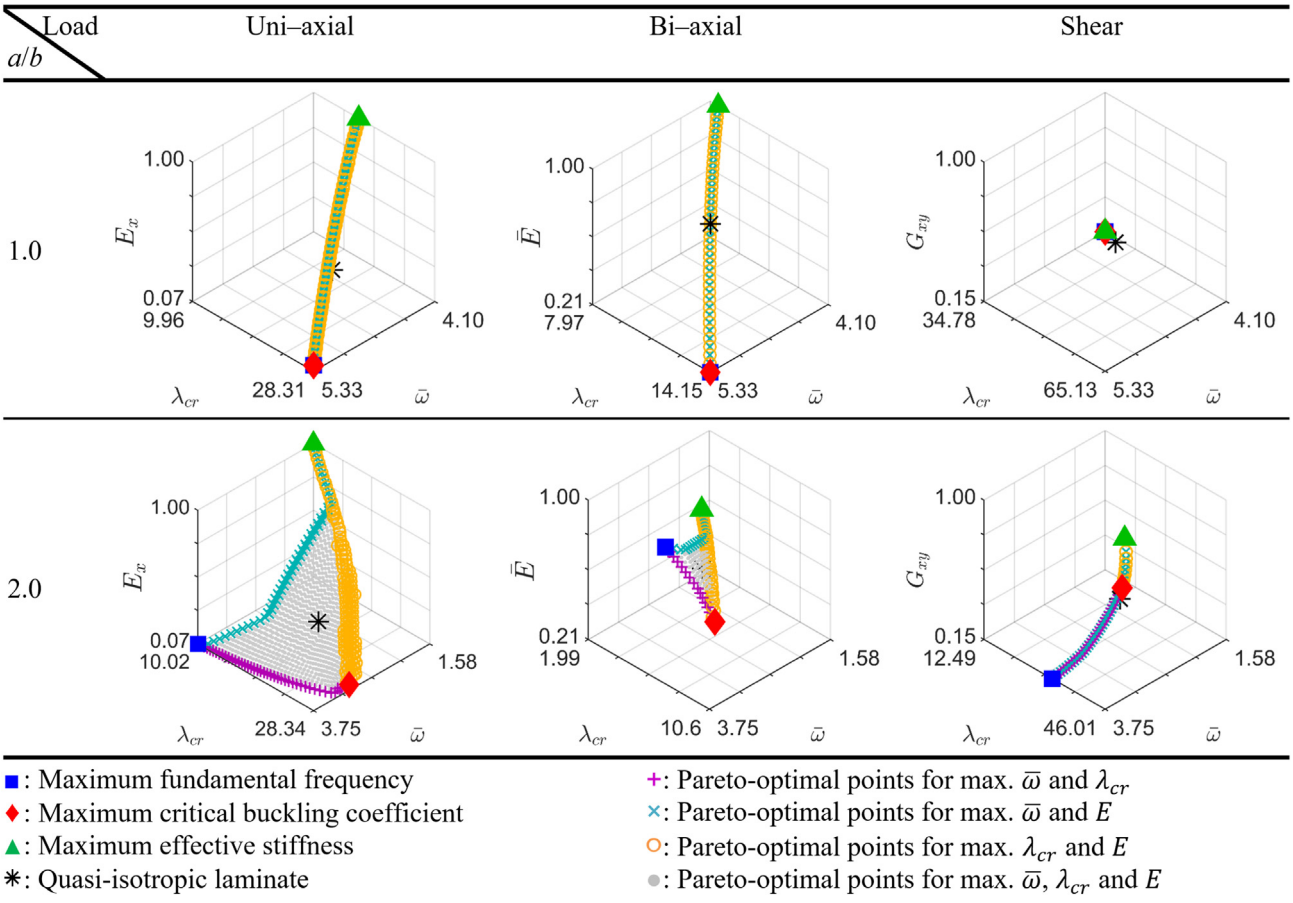


Fig. 12. 2-objective and 3-objective Pareto fronts for maximum fundamental frequency, critical buckling coefficient and effective stiffnesses considering simply-supported panels subjected to different loadings.

simply-supported panels. The rows show the results for different panel aspect ratios where the columns represent different load cases. The optimal point markers for the individual metrics remain the same as in the previous cases (see Figs. 3, 6, 8, 10). The quasi-isotropic laminate point is marked by black asterisk (✳). 2-objective Pareto-optimal points excluding the individual optimal points are designated by magenta plus signs (+) for maximum fundamental frequency & buckling load, cyan cross signs (×) for maximum fundamental frequency & effective stiffness, and orange rings (○) for maximum buckling load & effective stiffness. Pareto-optimal points for maximization of all three objectives are shown by grey circles (●). The marker types are selected such that when multiple points coincide, they can still be discerned in the figures.

For the square plate ($a/b = 1.0$), optimum point is ($V_1^{opt} = 0.0, V_3^{opt} = -1.0$) for both fundamental frequency and critical buckling coefficient for all load cases. However, when maximum effective stiffness is also considered, Pareto sets form except for the shear loading where the optimal point for all metrics is the same. The 2-objective Pareto-optimal points are a subset of 3-objective Pareto sets, meaning that there are also 3-objective Pareto-optimal points behind all 2-objective Pareto sets. Note that, the Pareto sets may contain points at the inner region of the feasible domain. Since the interior points require at least two layer angles, a stacking-sequence retrieval process is required for those points. This characteristic of the multi-objective optimization solutions is clearly different than that of single-objective solutions which ordinarily require single-angle laminates as shown in the previous section and also demonstrated by Grenestedt [34]. The interior Pareto-optimal points are located around the line interpolating the individual optimum points for the square plate.

When a/b ratio becomes 2.0, different requirements of individual performance metrics cause the Pareto sets to be considerably enlarged.

Table 6
Relative to the baseline values, the percentage changes in the fundamental frequency ($\overline{\omega}$), critical buckling coefficient (λ_{cr}) and effective stiffness (E) at the optimal point of each metric considering simply-supported panels.

		$a/b = 1.0$			$a/b = 2.0$		
Design point	Metric	Uni-axial	Bi-axial	Shear	Uni-axial	Bi-axial	Shear
$\overline{\omega}^{opt}$	$\overline{\omega}$	12.21%	12.21%	12.21%	25.42%	25.42%	25.42%
	λ_{cr}	25.49%	25.44%	21.49%	−55.32%	5.64%	−18.11%
	E	−70.65%	−70.64%	73.91%	−80.26%	39.86%	−74.09%
λ_{cr}^{opt}	$\overline{\omega}$	12.21%	12.21%	12.21%	−55.52%	22.07%	15.38%
	λ_{cr}	25.49%	25.44%	21.49%	25.12%	49.51%	20.07%
	E	−70.65%	−70.64%	73.91%	−70.65%	−28.37%	44.35%
E^{opt}	$\overline{\omega}$	−13.68%	−13.68%	12.21%	−47.16%	−3.68%	3.34%
	λ_{cr}	−25.53%	−25.53%	21.49%	−55.76%	−6.91%	7.57%
	E	159.74%	41.84%	73.91%	159.74%	41.84%	73.91%

For this aspect ratio, 3-objectives Pareto sets contain additional points, which are not present in the Pareto sets belonging to each binary combination of design objectives. These 3-objective Pareto sets appear to be a "filled" version of a frame consisting of 3 edges which are actually the binary Pareto sets. Note that, the binary Pareto sets can be considered as edges since the individual objectives are connected by the Pareto-optimal points is due to continuous response surfaces. When individual optimum points are located far away from each other, such as for panel with aspect ratio 2.0 under uni-axial loading, the Pareto set gets too crowded and fill nearly entire design space. Another important point is that, the maximum fundamental frequency and maximum buckling load designs are different for $a/b = 2.0$. This shows that, the fundamental frequency and buckling load metrics should be individually considered in the design stage, even though they are correlated. For these metrics, the Pareto-optimal points are located on the boundary of Miki's diagram. Hence, each point corresponds to a specific laminate angle which lie on the intervals: [±45°,90°], [±71.12°,90°], [±58.28°,90°] for uni-axial, bi-axial and shear loading, respectively. The Pareto sets for maximum fundamental frequency and effective stiffness are located around the upper boundary of Miki's diagram which corresponds to laminates with different ratios of 0° and 90° layers. For maximum buckling coefficient and effective stiffness metrics, sharp corners in the optimal solution distributions occur for uni-axial and bi-axial loading. This behavior is a result of the kinks on critical buckling coefficient response surface originating from the change of critical buckling mode indices (see Section 3.2).

Note that, optimum design for the maximum natural frequency may change due to pre-stressing effects caused by the loading used for the buckling and static analyses. However, under real operating conditions, the loading may fluctuate and even change sign. Therefore, it is reasonable to consider the unstressed panels for the fundamental frequency maximization.

Fig. 12 shows Pareto fronts in objective function space for binary and ternary combinations of maximum fundamental natural frequency, buckling load and effective stiffness considering simply-supported panels. These plots demonstrate how the value of each metric changes along the Pareto set. By choosing a Pareto-optimal point, the designer makes a compromise between the values of individual performance metrics. Note that, the axis limits in Pareto front plots are set to minimum and maximum values of each metric.

In Table 6, the percentage changes in the fundamental frequency, critical buckling coefficient and effective stiffness metrics of the simply-supported panels are presented for the optimal point of each metric. The rows of the first column stand for the design point in consideration. The sub-rows contain the percentage changes for the specified performance metrics compared to the baseline values. Note that the baseline laminate configuration is selected as quasi-isotropic laminate with ($V_1 = 0.0, V_3 = 0.0$). The results show that the optimal solutions for different performance metrics can strongly conflict each other, as the increase in a certain metric can lead to a significant decrease in another one. Thus, finding Pareto sets for such multi-objective laminate optimization problems is important to detect all the optimal solution candidates and find the best compromise among them.

4.2. Clamped panels

Fig. 13 shows Pareto-optimal points for maximum fundamental frequency, critical buckling coefficient and effective stiffnesses considering

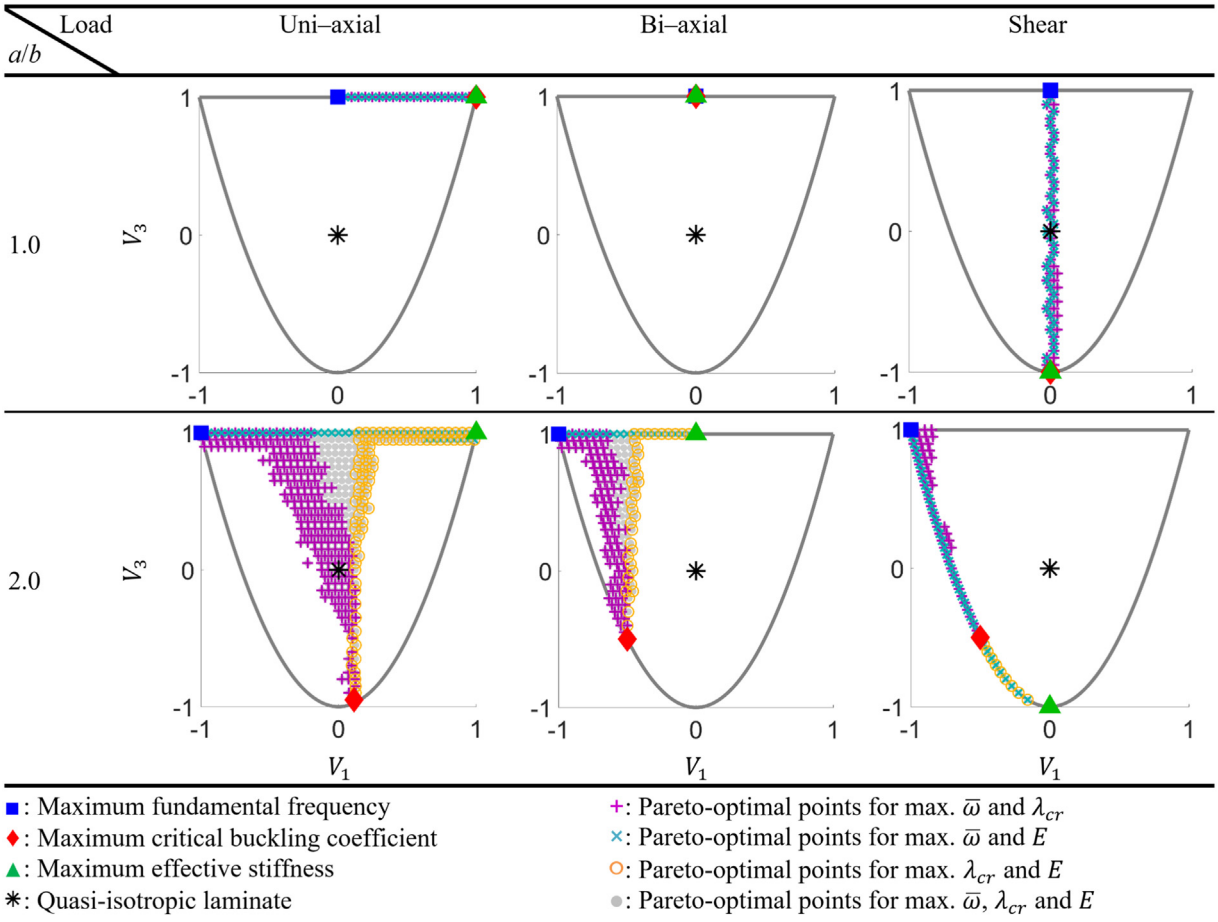


Fig. 13. 2-objective and 3-objective Pareto-optimal design points for maximum fundamental frequency, critical buckling coefficient and effective stiffnesses considering clamped panels subjected to different loadings.

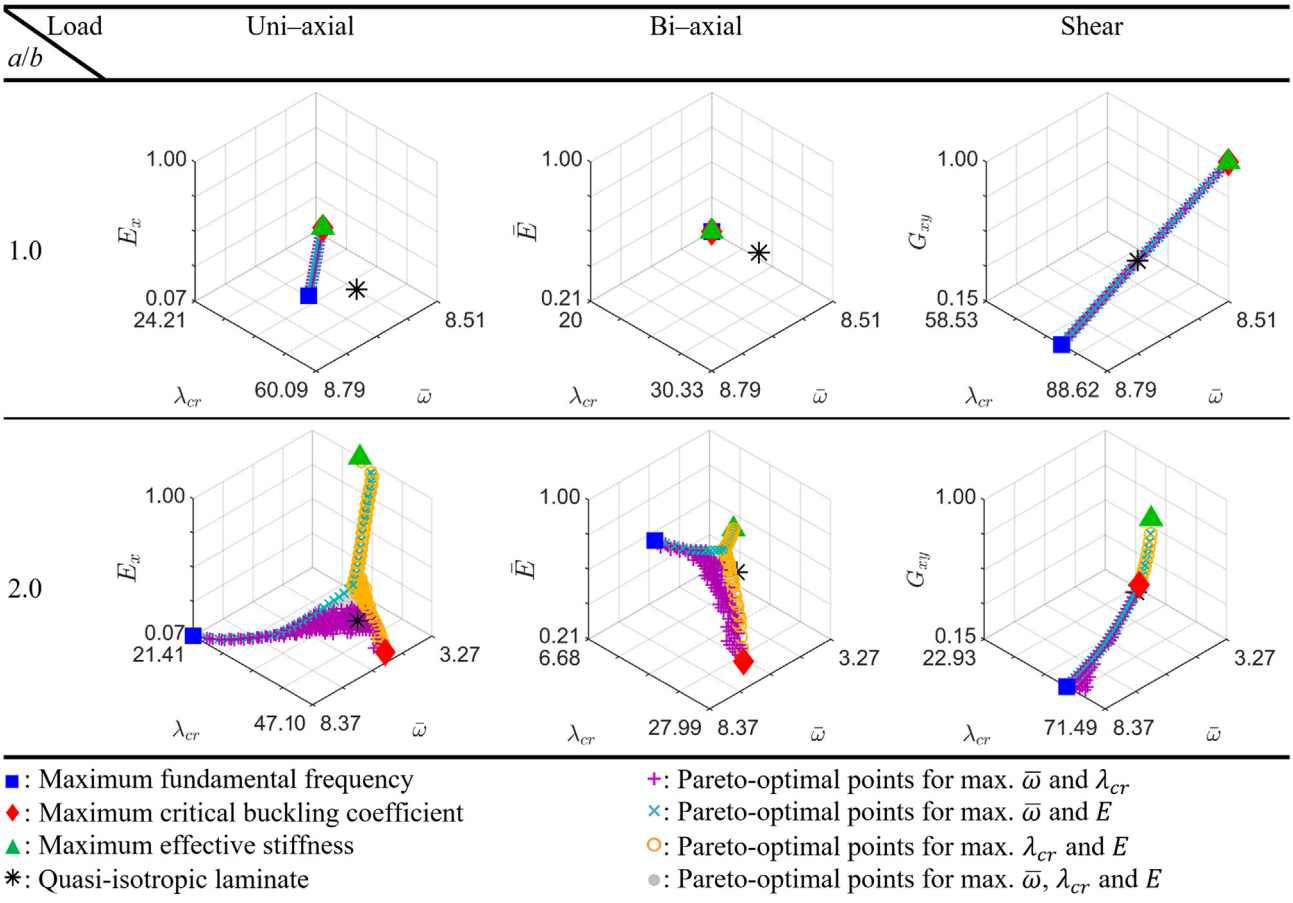


Fig. 14. 2-objective and 3-objective Pareto fronts for maximum fundamental frequency, critical buckling coefficient and effective stiffnesses considering clamped panels subjected to different loadings.

clamped panels. Although their distribution is different compared to simply-supported panels, the large Pareto sets also appear for this case. Only for the square panels under bi-axial loading, a single optimum point is found.

For clamped boundary conditions, the conflict between the maximum fundamental frequency and maximum critical buckling coefficient points is greater. This fact can be seen by examining the different optimal points required to maximize these two metrics for the square panels under uni-axial and shear loading, which were the same for simply-supported plates. In addition, unlike simply-supported plates, the Pareto-optimal points for maximum fundamental frequency and buckling load do not always lie on the boundary of Miki's diagram. For the square clamped plates, the Pareto-optimal solutions for maximum fundamental frequency and effective stiffness are located around the line interpolating the individual optimum points. For these panels, optimal points for maximum buckling load and effective stiffness metrics are the same for all loading cases.

For $a/b = 2.0$, Pareto-optimal solutions involving buckling load metric significantly deviate from the line that interpolates lamination parameter values for individual optimum points, when uni-axial and bi-axial loads are considered. In such cases, the major portion of Pareto-optimal solutions is located at the interior of Miki's diagram, which shows that single-angle designs perform poorly. Therefore, obtaining the Pareto sets with a sufficient resolution of lamination parameter increments is clearly important for the detection of the all optimal solutions within the feasible domain. Note that, while retrieving an actual

Table 7
Relative to the baseline values, the percentage changes in the fundamental frequency ($\overline{\omega}$), critical buckling coefficient (λ_{cr}) and effective stiffness (E) at the optimal point of each metric considering clamped panels.

		$a/b = 1.0$			$a/b = 2.0$		
Design point	Metric	Uni-axial	Bi-axial	Shear	Uni-axial	Bi-axial	Shear
$\overline{\omega}^{opt}$	$\overline{\omega}$	1.38%	1.38%	1.38%	39.50%	39.50%	39.50%
	λ_{cr}	1.36%	0.09%	−7.61%	−52.24%	−19.79%	−8.71%
	E	41.82%	41.84%	−74.09%	−80.26%	39.86%	−74.09%
λ_{cr}^{opt}	$\overline{\omega}$	1.20%	1.38%	−1.85%	12.33%	15.50%	15.50%
	λ_{cr}	5.14%	0.09%	5.99%	5.06%	22.28%	16.57%
	E	159.74%	41.84%	73.91%	−62.08%	−48.23%	36.87%
E^{opt}	$\overline{\omega}$	1.20%	1.38%	−1.85%	−45.50%	6.50%	−7.50%
	λ_{cr}	5.14%	0.09%	5.99%	−29.47%	4.67%	2.84%
	E	159.74%	41.84%	73.91%	159.74%	41.84%	73.91%

laminate configuration for the inner Pareto-optimal points, certain points can be preferable over the others due to manufacturing constraints.

In Fig. 14, Pareto fronts in objective function space for binary and ternary combinations of maximum fundamental natural frequency, buckling load and effective stiffness are presented for clamped plates. One can see that increasing the aspect ratio generally increases the conflict between the individual optimal designs, which was also the case for simply-supported boundary plates. This condition makes the design points spread away enlarging the size of Pareto sets.

In Table 7, the percentage changes in the fundamental frequency, critical buckling coefficient and effective stiffness metrics of the clamped panels are presented for the optimal point of each metric. Compared to simply-supported plates, the difference between the maximum fundamental frequency and the quasi-isotropic design frequency is smaller (1.38% vs. 12.21%) for square clamped plate and greater (39.50% vs. 25.42%) for clamped plate with $a/b = 2.0$. Maximization of buckling load provides lesser improvement percentages in all cases.

5. Conclusions

In this paper, a multi-objective design methodology was presented for maximizing the fundamental frequency, buckling load and effective stiffness of laminated composite plates. Lamination parameters were used to characterize the stiffness properties in a compact form which also provided a convex design space for the optimization problem. The study contributes to the literature with an extensive investigation of multi-objective optimization solutions computed in lamination parameter domain for different combinations of design objectives.

Firstly, analyses were performed to get responses for individual performance metrics as a function of lamination parameters by using full-factorial search and, single-objective optimal designs were determined for various problem cases. The results were displayed by showing the response surfaces and optimal points on Miki's lamination diagram. Then, multi-objective optimization studies were carried out where the trends of the objective functions with respect to design variables were observed to be conflicting for several problem types. For these cases, Pareto-optimal solutions were calculated to obtain sets of non-dominated designs. The distributions of Pareto sets in lamination parameter space, which are notably informative for multi-objective optimization studies, were presented. The results showed that, Pareto-optimal solutions reflect the features in the contours of the investigated metrics such as sharp changes. Even though individual optimum solutions lie on the boundary of Miki's diagram, Pareto-optimal solutions do not necessarily follow this trend. Therefore, searching the interior region of the feasible domain is particularly important in multi-objective optimization problems. In addition, Pareto-optimal solutions may deviate from the line interpolating the individual optimal solution parameters. For 3-metric optimization problem, the Pareto sets appeared to be a "filled" version of the closed-loop consisting of the Pareto sets belonging to each binary combinations of design objectives. Hence, when all the binary solutions are strongly conflicting, resulting Pareto sets may be too crowded covering almost the entire design space. The Pareto fronts revealed that, increasing the aspect ratio generally increases the conflict between different metrics.

Finally, the values of the fundamental frequency, buckling load and effective stiffness metrics at the optimal point of each metric were investigated. The analyses revealed that the optimal solutions for different performance metrics could strongly conflict with each other, as the increase in a certain metric could lead to a significant decrease in another one. This result demonstrated the importance of finding Pareto sets for multi-objective laminate optimization problems to detect all the optimal solution candidates and find the best compromise among them.

The focus of this work was on building a multi-objective optimization framework for composite plates based on lamination parameters. Having provided significantly interesting and informative results, the developed framework can certainly be utilized for other boundary conditions, load cases and/or panel geometries in the future studies. Retrieval of stacking-sequence is another potential research direction, which can require additional restrictions on available layer thicknesses, volumetric percentage of layers with certain angles and/or change of angle between adjacent layers. Such investigation can show the degree of conformity between the properties of the actual laminate configuration and optimal design in lamination parameter domain.

CRediT author statement

Gokhan Serhat: Developed the methodology, programmed the necessary software scripts, performed the simulations, prepared the figures and wrote the manuscript. **Ipek Basdogan**: Supervised the project and revised the manuscript.

Acknowledgments

The authors would like to gratefully acknowledge the funding from European Union Seventh Framework Programme "FP7-PEOPLE-2012-ITN" under grant agreement 316394, through the Marie Curie Initial Training Network "Aerospace Multidisciplinarity Enabling DEsign Optimization (AMEDEO)".

Declaration of Competing Interest

The authors declare no competing interests.

Data availability

The raw/processed data required to reproduce these findings cannot be shared at this time due to technical or time limitations.

References

[1] C.W. Bert, Optimal design of composite material plates to maximize its fundamental frequency, J. Sound Vib. 50 (1977) 229–237, https://doi.org/10.1016/0022-460X(77)90357-1.
[2] Y. Narita, P. Robinson, Maximizing the fundamental frequency of laminated cylindrical panels using layerwise optimization, Int. J. Mech. Sci. 48 (2006) 1516–1524, https://doi.org/10.1016/j.ijmecsci.2006.06.008.
[3] M.K. Apalak, M. Yildirim, R. Ekici, Layer optimisation for maximum fundamental frequency of laminated composite plates for different edge conditions, Compos. Sci. Technol. 68 (2008) 537–550, https://doi.org/10.1016/j.compscitech.2007.06.031.
[4] Y. Hirano, Optimum design of laminated plates under axial compression, AIAA J. 17 (1979) 1017–1019, https://doi.org/10.2514/3.61269.
[5] H.T. Hu, B.H. Lin, Buckling optimization of symmetrically laminated plates with various geometries and end conditions, Compos. Sci. Technol. 55 (1995) 277–285, https://doi.org/10.1016/0266-3538(95)00105-0.
[6] O. Erdal, F.O. Sonmez, Optimum design of composite laminates for maximum buckling load capacity using simulated annealing, Compos. Struct. 71 (2005) 45–52, https://doi.org/10.1016/j.compstruct.2004.09.008.
[7] T.Y. Kam, F.M. Lai, Maximum stiffness design of laminated composite plates via a constrained global optimization approach, Compos. Struct. 32 (1995) 391–398, https://doi.org/10.1016/0263-8223(95)00070-4.
[8] Z. Gürdal, B.F. Tatting, C.K. Wu, Variable stiffness composite panels: effects of stiffness variation on the in-plane and buckling response, Compos. Part A Appl. Sci. Manuf. 39 (2008) 911–922, https://doi.org/10.1016/j.compositesa.2007.11.015.
[9] H. Fukunaga, H. Sekine, Optimal design of symmetric laminated plates for fundamental frequency, J. Sound Vib. 171 (1994) 219–229, https://doi.org/10.1006/jsvi.1994.1115.
[10] C.G. Diaconu, M. Sato, H. Sekine, Layup optimization of symmetrically laminated thick plates for fundamental frequencies using lamination parameters, Struct. Multidiscip. Optim. 24 (2002) 302–311, https://doi.org/10.1007/s00158-002-0241-z.
[11] G. Serhat, I. Basdogan, Design of curved orthotropic composite panels for optimal frequency-response using lamination parameters, Compos. Part B Eng. 147 (2018) 135–146, https://doi.org/10.1016/j.compositesb.2018.04.033.
[12] M.M. Abdalla, S. Setoodeh, Z. Gürdal, Design of variable stiffness composite panels for maximum fundamental frequency using lamination parameters, Compos. Struct. 81 (2007) 283–291, https://doi.org/10.1016/j.compstruct.2006.08.018.
[13] G. Serhat, I. Basdogan, Lamination parameter interpolation method for design of manufacturable variable-stiffness composite panels, AIAA J. (2019)https://doi.org/10.2514/1.J057902.

[14] H. Fukunaga, H. Sekine, M. Sato, et al., Buckling design of symmetrically laminated plates using lamination parameters, Comput. Struct. 57 (1995) 643–649, https://doi.org/10.1016/0045-7949(95)00050-Q.
[15] J.L. Grenestedt, Layup optimization against buckling of shear panels, Struct. Optim. 3 (1991) 115–120, https://doi.org/10.1007/BF01743281.
[16] S.T. Ijsselmuiden, M.M. Abdalla, Z. Gürdal, Optimization of variable-stiffness panels for maximum buckling load using lamination parameters, AIAA J. 48 (2010) 134–143, https://doi.org/10.2514/1.42490.
[17] H. Fukunaga, H. Sekine, Stiffness design method of symmetric laminates using lamination parameters, AIAA J. 30 (1992) 2791–2793, https://doi.org/10.2514/3.11304.
[18] M. Miki, Y. Sugiyama, Optimum design of laminated composite plates using lamination parameters, AIAA J. 31 (1993) 921–922, https://doi.org/10.2514/3.49033.
[19] S. Setoodeh, M. Abdalla, Z. Gürdal, Design of variable-stiffness laminates using lamination parameters, Compos. Part B Eng. 37 (2006) 301–309, https://doi.org/10.1016/j.compositesb.2005.12.001.
[20] T.Y. Kam, R.R. Chang, Design of laminated composite plates for maximum buckling load and vibration frequency, Comput. Methods Appl. Mech. Eng. 106 (1993) 65–81, https://doi.org/10.1016/0045-7825(93)90185-Z.
[21] M. Abouhamze, M. Shakeri, Multi-objective stacking sequence optimization of laminated cylindrical panels using a genetic algorithm and neural networks, Compos. Struct. 81 (2007) 253–263, https://doi.org/10.1016/j.compstruct.2006.08.015.
[22] M.A. Nik, K. Fayazbakhsh, D. Pasini, et al., Surrogate-based multi-objective optimization of a composite laminate with curvilinear fibers, Compos. Struct. 94 (2012) 2306–2313, https://doi.org/10.1016/j.compstruct.2012.03.021.
[23] G. Serhat, T.G. Faria, I. Basdogan, Multi-objective optimization of stiffened, fiber-reinforced composite fuselages for mechanical and vibro-acoustic requirements, Proceedings of 17th AIAA/ISSMO Multidisciplinary Analysis and Optimization Conference, AIAA, Washington, DC, 2016https://doi.org/10.2514/6.2016-3509.
[24] S.W. Tsai, H.T. Hahn, Introduction to Composite Materials, Technomic, Lancaster, 1980.
[25] J.L. Grenestedt, P. Gudmundson, Layup optimization of composite material structures, in: P. Pedersen (Ed.), Proceedings of IUTAM Symposium on Optimal Design with Advanced Materials, Elsevier Science, Amsterdam 1993, pp. 311–336.
[26] G. Serhat, I. Basdogan, Comparison of vibro–acoustic performance metrics in the design and optimization of stiffened composite fuselages, in: W. Kropp, O. von Estorff, B. Schulte-Fortkamp (Eds.), Proceedings of 45th International Congress and Exposition on Noise Control Engineering, Curran Associates, New York 2016, pp. 6079–6090.
[27] Z. Gürdal, R.T. Haftka, P. Hajela, Design and Optimization of Laminated Composite Materials, John Wiley & Sons, New York, 1999.
[28] H. Fukunaga, G.N. Vanderplaats, Stiffness optimization of orthotropic laminated composites using lamination parameters, AIAA J. 29 (1991) 641–646, https://doi.org/10.2514/3.59931.
[29] M. Miki, Design of laminated fibrous composites plates with required flexural stiffness, in: J. Carlsson, N.G. Ohlson (Eds.), Proceedings of the Fourth International Conference, Pergamon Press, Oxford 1984, pp. 465–471.
[30] G.R. Liu, S.S. Quek, The Finite Element Method: A Practical Course, Butterworth-Heinemann, Oxford, 2003.
[31] R.G. Anderson, B.M. Irons, C. Zienkiewicz, Vibration and stability of plates using finite elements, Int. J. Solids Struct. 4 (1968) 1031–1055, https://doi.org/10.1016/0020-7683(68)90021-8.
[32] G. Serhat, I. Basdogan, Effect of aspect ratio and boundary conditions on the Eigen frequency optimization of composite panels using lamination parameters, in: J.D. Müller, et al., (Eds.), Proceedings of 11th ASMO-UK/ISSMO/NOED2016 International Conference on Numerical Optimisation Methods for Engineering Design, ASMO-UK, Leeds 2017, pp. 160–168.
[33] K. Deb, Multi-objective Optimization Using Evolutionary Algorithms, John Wiley & Sons, New York, 2001.
[34] J.L. Grenestedt, Composite plate optimization only requires one parameter, Struct. Optim. 2 (1990) 29–37, https://doi.org/10.1007/BF01743518.